

# Increase Coherent Time in Plasmonic System by Spectral Hole Burning Effect

Jia-Bin You,<sup>1,\*</sup> Xiao Xiong,<sup>1</sup> Ping Bai,<sup>1</sup> Zhang-Kai Zhou,<sup>2</sup> Wan-Li Yang,<sup>3</sup> Ching Eng Png,<sup>1</sup> and Lin Wu<sup>1,†</sup>

<sup>1</sup>*Institute of High Performance Computing, A\*STAR (Agency for Science, Technology and Research), 1 Fusionopolis Way, #16-16 Connexis, Singapore 138632*

<sup>2</sup>*State Key Laboratory of Optoelectronic Materials and Technologies, School of Physics, Sun Yat-sen University, Guangzhou 510275, China*

<sup>3</sup>*State Key Laboratory of Magnetic Resonance and Atomic and Molecular Physics, Wuhan Institute of Physics and Mathematics, Chinese Academy of Sciences, Wuhan 430071, P. R. China*

The plasmonic systems suffer from a significant degree of decoherence from the intrinsic large dissipative and radiative damping mechanisms. Here we demonstrate that this restrictive drawback can be mitigated by hybridizing the plasmonic system with an emitter ensemble of inhomogeneously-broadened transition frequencies. We find that the coherent time of Rabi oscillation of the hybrid system is significantly increased by burning two narrow spectral holes in the spectral density of the emitter ensemble. The spectral hole burning technique paves the way for the practical use of the hybrid quantum plasmonic systems for the processing of quantum information.

*Introduction.*- Plasmonics provides a unique system for manipulating light via the confinement of the electromagnetic field to regions well beyond the diffraction limit of light [1–3]. This has opened up a wide range of applications based on extreme light confinement [4], including optical metamaterials [5], biosensing [6] and nanoantennas [7]. However, a significant part of the energy of the system is dissipated via the plasmonic losses which present a major hurdle in the development of plasmonic devices and circuits that can compete with other mature technologies. Recently, there has been a growing excitement about the prospects for exploring quantum properties of plasmonic polaritons and building plasmonic devices that is strongly coupled to an ensemble of quantum emitters [8–10]. The hybrid integration shows its potential to bypass individual weakness while harnessing their strength. In particular, it helps to reduce dissipation of the plasmonic polaritons and also makes possible the entering into strong coupling regime for the plasmonic system at room temperature. The strong coupling can enable quantum information to be transmitted over longer distance or processed for a longer time, which is essential for quantum communication and computation [1, 2].

Recently, the strong coupling has already been realized in the hybrid plasmonic devices [8–10]. However, there are two bottlenecks for the processing of quantum information in these hybrid quantum systems. On one hand, the intrinsic large decay of the plasmonic polariton will shorten the coherent time of the system; on the other hand, the inhomogeneous broadening of the emitter ensemble, i.e., the different transition frequencies between each emitter, will further increase the broadening of the hybridized polariton peak.

Previously, there have been two approaches to resolve this problem in the microwave cavity systems. It was shown that the decoherence is naturally suppressed for

very strong coupling when the spectral density of ensemble falls off sufficiently fast in its tails. This so-called “cavity protection effect” [11–13] has been observed experimentally [14]. However, it requires very high value of the coupling strength, which is presently difficult to access experimentally. Furthermore, the large decay rate of plasmon is the minimally reachable value for the decay rate of the polariton peak [12].

An alternative approach is the spectral hole burning (SHB) technique which is based on collective dark states [15] that circumvents the necessity of very high coupling strength and substantially improves the coherent time of the system beyond the limit given by the individual cavity or emitter ensemble. The SHB is a frequency selective bleaching technique, which leads to an increased transmission at the burned spectral hole of the selected frequency. To observe this phenomenon, firstly, the spectral density of ensemble should be inhomogeneously broadened; and secondly, the spectral density should undergoes a modification which changes the transmission spectrum of the system. Typical emitters include dye molecules dissolved in suitable host matrices [16]. The SHB effect has been purposed for the realization of the high-density frequency domain optical storage [17], high-resolution spectroscopy [18], slow light effect [19] and quantum information processing [20] which has been experimentally realized in the microwave domain [15].

In this work, we explore the SHB effect in a hybrid plasmonic nanocavity system for mitigating the notorious large decay of plasmonic system in the bad cavity region. The cavity is coupled to an emitter ensemble with transition frequencies distributed in a frequency comb. By investigating the transmission spectrum via the matrix product state (MPS) algorithm, we identify the SHB effect by a pair of narrow broadening peaks which originates from the collective dark states. The decay rate of this hybridized polariton peak can even be substantially smaller than the decay rate of the original plasmonic cavity. We then use the time-dependent variational principle (TDVP) to evolve the system in time and observe the Rabi oscillation of the system. It is found that the co-

\* you\_jiabin@ihpc.a-star.edu.sg

† wul@ihpc.a-star.edu.sg

herent time of the hybrid plasmonic system is remarkably enhanced after SHB. The Rabi frequency is determined by the position of the spectral holes which is tunable by the modulation frequency of hole burning pulse [15]. An added advantage for the frequency comb setup is that the SHB effect can be observed in a small emitter ensemble ( $N \sim 50$ ) while a large emitter ensemble ( $N \sim 5000$ ) is needed for randomly-distributed transition frequencies. We then propose a pumping scheme for the hybrid plasmonic system to observe the SHB effect. It is found that instead of the constant driving scheme, the periodical driving can excite the system efficiently so that the SHB effect can be clearly observed. We also discuss the SHB effect in the presence of imperfection of frequency comb and for the emitter ensemble with randomly-distributed transition frequencies.

*Model.*- In Fig. 1(a), the plasmonic cavity is coupled by an emitter ensemble which contains  $N$  quantum emitters modeled as two-level systems with transition frequencies  $\omega_i$  and transition operator  $\sigma_i^+ = |e_i\rangle\langle g_i|$  between ground state  $|g_i\rangle$  and excited state  $|e_i\rangle$ . The plasmonic cavity, with resonant frequency  $\omega_a$ , is second quantized and described by a quantum harmonic oscillator with the bosonic creation (annihilation) operator  $a^\dagger(a)$  with canonical commutation relation  $[a, a^\dagger] = 1$ . Each emitter couples with the plasmonic cavity mode through the Jaynes-Cummings interaction with coupling strength  $g_i$ . A laser field  $E_L(t)$  with probing frequency  $\omega$  pumps the entire system via the dipole moments of cavity  $\mu_a$  and emitters  $\mu_e$  with the strengths  $\Omega_a(t) = \mu_a E_L(t)$  and  $\Omega_e(t) = \mu_e E_L(t)$ . In a rotating frame with probing frequency  $\omega$ , the Hamiltonian of the system can be recast into

$$H = \Delta_a a^\dagger a + \sum_{i=1}^N [\Delta_i \sigma_i^+ \sigma_i^- + g_i (\sigma_i^+ a + a^\dagger \sigma_i^-)] + \Omega_a(t)(a + a^\dagger) + \Omega_e(t)(S^- + S^+), \quad (1)$$

where  $S^- = \sum_{i=1}^N \sigma_i^-$  and the laser detunings for the cavity and emitters are given by  $\Delta_a = \omega_a - \omega$  and  $\Delta_i = \omega_i - \omega$  respectively. In general, the energies of the cavity and the emitters are inevitably dissipated into the surrounding environment, its dynamics is governed by the master equation for an open system [21]

$$\partial_t \rho = i[\rho, H] + \frac{\kappa}{2} \mathcal{D}[a]\rho + \frac{\Gamma}{2} \sum_i \mathcal{D}[\sigma_i^-]\rho, \quad (2)$$

where  $\rho$  is the density matrix of the system and  $\mathcal{D}[\hat{o}]\rho = 2\hat{o}\rho\hat{o}^\dagger - \hat{o}^\dagger\hat{o}\rho - \rho\hat{o}^\dagger\hat{o}$  is the Lindblad term which accounts for the losses from both cavity and emitters with decay rates  $\kappa$  and  $\Gamma$  respectively.

*Spectral hole burning effect.*- To interpret the spectral hole burning effect, we first consider a simplified case where the coherent driving field only acts on the plasmonic cavity ( $\Omega_e(t) = 0$ ). In the limit of low driving intensity when the linear approximation,  $\langle \sigma_{i,z} \rangle \approx -1$ ,

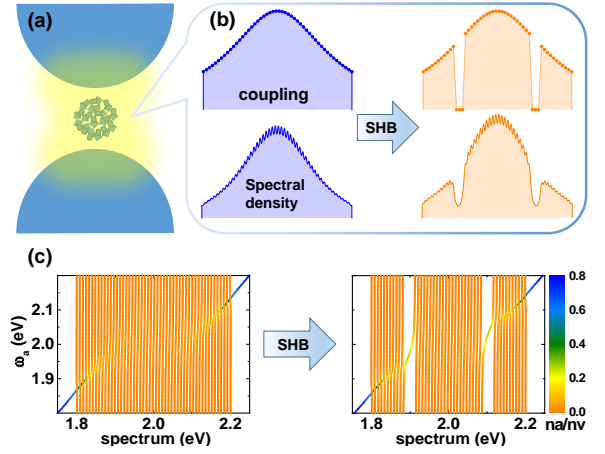


FIG. 1. (a) hybrid system of plasmonic cavity strongly coupled to an inhomogeneously broadened emitter ensemble. (b) the individual coupling strengths between cavity and ensemble, and the spectral density of the emitter ensemble before and after the SHB. (c) single-excitation spectra of the system before and after SHB, where the population of cavity photon is indicated by the colour bar in the right.

is valid, we can derive the equations of motion for the system,

$$\begin{aligned} \langle \dot{a} \rangle &= -(i\Delta_a + \kappa/2)\langle a \rangle - i \sum_i g_i \langle \sigma_i^- \rangle - i\Omega_a(t), \\ \langle \dot{\sigma}_i^- \rangle &= -(i\Delta_i + \Gamma/2)\langle \sigma_i^- \rangle - ig_i \langle a \rangle. \end{aligned} \quad (3)$$

After straightforward calculations, we find that the transmission spectrum of the hybrid plasmonic system  $T(\omega)$ , which is proportional to the emitted photon number of the cavity,  $\langle a^\dagger a \rangle$ , is given by

$$T(\omega) \propto \left| \frac{1}{\Delta_a - \Omega^2 \delta(\omega) - i[\kappa + \Omega^2 \rho(\omega)]/2} \right|^2. \quad (4)$$

Here the mean-field approximation,  $\langle a^\dagger a \rangle \approx |\langle a \rangle|^2$ , has been used. We observe that the resonant frequency and spectral broadening of the plasmonic cavity can be modified by the dressed emitter ensemble. In particular, the resonant frequency  $\omega_a$  is shifted by the Lamb shift  $\Omega^2 \delta(\omega) = \sum_i \frac{g_i^2}{(\Gamma/2)^2 + \Delta_i^2} \Delta_i$  and the spectral broadening  $\kappa$  is increased by an amount of the density of states of the emitter ensemble,  $\Omega^2 \rho(\omega) = \sum_i \frac{g_i^2}{(\Gamma/2)^2 + \Delta_i^2} \Gamma$ . Here  $\Omega^2 = \sum_i g_i^2$  is the effective coupling strength which is enhanced by a factor of  $\sqrt{N}$  compared to the single coupling strength,  $g_i$ , so that the strong coupling in the hybrid plasmonic system can be reached.

Based on the transmission spectrum Eq. (4), we now demonstrate that by judiciously choosing the property of emitter ensemble, the spectral hole burning effect can increase the coherent time of the Rabi oscillation of the system. First we consider the case where the emitters in the ensemble are arranged in a finite frequency comb [22] with transition frequencies spaced at

equidistant intervals. Specifically, the transition frequencies  $\omega_i = \omega_e - \Delta\omega + \frac{2\Delta\omega}{N-1}(i-1)$  are equally arranged in the range of  $[\omega_e - \Delta\omega, \omega_e + \Delta\omega]$ , ( $i = 1, 2, \dots, N$ ) centered at  $\omega_e$ . The coupling constants between each emitter and the cavity follow a  $q$ -Gaussian distribution  $g_i = Ae_q[-\beta(\omega_i - \omega_e)^2]$ , where  $e_q(x) = [1 + (1-q)x]^{\frac{1}{1-q}}$  and  $A$  is the amplitude [20, 23]. This leads to the  $q$ -Gaussian spectral density of ensemble shown in the left panel of Fig. 1(b) with the parameters  $q = 2$  and  $\beta = 0.1$ . We then apply a hole burning pulse on the emitter ensemble. When the pulse intensity is above a certain power threshold, it will thermalize emitters of selected frequency into an equal mixture of their ground and excited states and so cancels out their coherent light-matter interaction [15]. This will leave two symmetric spectral holes centered at around  $\omega_e \pm \Omega$  with a width of 33meV in the spectral density of ensemble  $\rho(\omega)$  as shown in the right panel of Fig. 1(b). The effect of hole burning can be further seen from the single-excitation energy spectrum. In Fig. 1(c), the energy spectra are plotted by sweeping the resonant energy of cavity  $\omega_a$ . It is found that after hole burning, two states emerge right within the spectral gaps and are isolated from the remaining subradiant states. These two states incorporated with the common ground state of the system, form an effective V-level structure that naturally hosts the dark states [24] which can significantly enhance the coherent time of the Rabi oscillation of the system.

*Rabi oscillation.*- To fully understand the behavior of the long-lived dark states in this hybrid quantum many-body system Eq. (2), we apply the variational MPS [25–30] and the TDVP algorithm [31, 32] to study the steady and dynamical properties of the system. By the Choi's representation [27], the master equation Eq. (2) can be recast into  $\partial_t |\rho\rangle\rangle = \mathcal{L}|\rho\rangle\rangle$ , where the density matrix  $\rho$  is reshaped into a column vector  $|\rho\rangle\rangle$  by concatenating all its columns and the Liouvillian superoperator is reformulated to operate on the enlarged space,

$$\mathcal{L} = i(H_{\text{eff}}^* \otimes I - I \otimes H_{\text{eff}}) + \kappa a \otimes a + \sum_i \Gamma \sigma_i^- \otimes \sigma_i^-, \quad (5)$$

where the effective Hamiltonian is obtained by the substitutions of  $\Delta_a \rightarrow \Delta_a - i\kappa/2$  and  $\Delta_i \rightarrow \Delta_i - i\Gamma/2$  in the original Hamiltonian  $H$  of Eq. (1). The determination of the steady density matrix can then be reformulated as the variational minimization [28] of the Euclidean norm functional  $|\mathcal{L}|\rho\rangle\rangle| \geq 0$  and the time evolution of the system can be achieved by the TDVP algorithm [32]. The expectation value of an observable  $\hat{O}$  can be obtained in Choi's representation by  $\langle \hat{O} \rangle = \text{tr}(\hat{O}\rho) = \langle\langle \hat{O}^\dagger |\rho\rangle\rangle$ .

We now discuss the spectral hole burning effect by the transmission spectrum of the plasmonic cavity  $T(\omega) \sim \langle a^\dagger a \rangle$ . It is observed that the SHB effect will significantly affect the emission of the hybrid plasmonic system as shown in the transmission spectrum  $T(\omega)$  in Fig. 2(a). Compared with the spectrum before the hole burn-

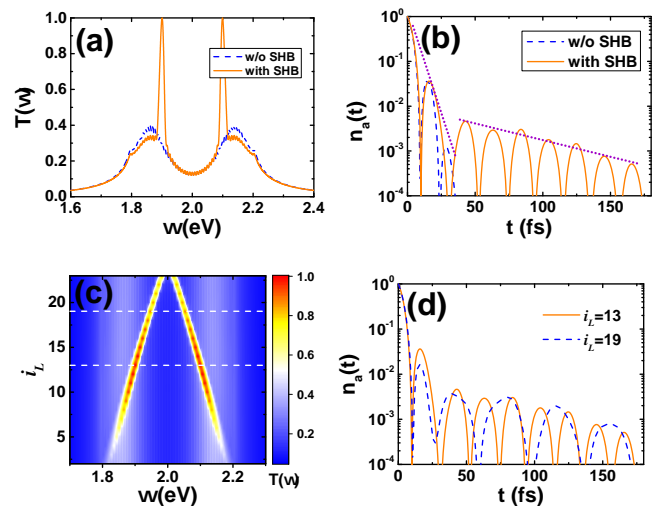


FIG. 2. SHB effect in a frequency comb. The cavity with frequency  $\omega_c = 2$  eV, is coupled with  $N = 50$  emitters, where the transition frequencies are distributed in a frequency comb centered at  $\omega_e = 2$  eV with a broadening of  $2\Delta\omega = 0.4$  eV. The coupling between individual emitter and cavity is followed by a  $q$ -Gaussian distribution parameterized by  $q = 2$  and  $\beta = 0.1$ . The decay rates for cavity and emitters are  $\kappa = 0.1$  eV and  $\Gamma = 0.01$  eV, respectively. The ratio of dipole moments of the cavity to the emitter is  $\mu_a = 19\mu_e$ . To demonstrate the SHB effect, two spectral holes are symmetrically burned at  $2 \pm 0.102$  eV with a width of 0.033 eV, which is equivalent to remove the emitters of positions  $i = 12, 13, 14, 37, 38, 39$  in the comb. The cavity is initially prepared in Fock state  $|1\rangle$  and the emitters are all in their ground states. (a) Normalized transmission spectrum with and without the SHB. (b) Rabi oscillation of cavity photon with and without the SHB. (c) Normalized transmission spectrum after SHB as a function of the centre of left hole  $i_L$  range from 1 to  $N/2$ . (d) tunable Rabi oscillations of cavity photon for different pairs of spectral holes. The holes for solid orange line is centred at  $(i_L, i_R) = (13, 38)$ , while the one for dashed blue line is centred at  $(i_L, i_R) = (19, 32)$ .

ing, we see that two sharp peaks emerge after the hole burning which are a direct evidence of formation of the collective dark states. The pair of dark states are well decoupled from the remaining subradiant states so that the broadening of the peaks are small compared to the background plasmonic polariton modes before burning. This reflects an advantage of the spectral hole burning. We find that the decay rates for the dark states  $\Gamma_D \approx 0.011$ eV can be well below the decay rate of the plasmonic cavity mode  $\kappa = 0.1$ eV. It only limits by the fundamental decay rate of single emitter  $\Gamma = 0.01$ eV. Thus this hybrid plasmonic system shows the potential to bypass the individual weaknesses of its subsystems. The advantage of this hybrid system can also be observed in the time domain. Compared with the background short-time Rabi oscillation, the small broadening of the dark states will establish a long-lived coherent Rabi oscillation. In Fig. 2(b), we initially excite the cavity in the

single-photon Fock state and de-excite the emitters in their ground states. It is found that after the background short-time oscillation, the long-lived oscillation resulting from the SHB will gradually emerge. The decay rate of the long-lived Rabi oscillation, which can be characterized by the slope, is about one magnitude smaller than that of the short-time Rabi oscillation. Thus the coherent time of the system is significantly prolonged by the hole burning. Furthermore, the pair of dark states is robust against the change of hole burning positions as shown in Fig. 2(c). It can be observed widely from 1.8 eV to 2.2 eV spectrally. However, there exist optimal burning positions centered at  $(i_L, i_R) = (13, 38)$  to achieve the most intensive peaks compared to the background spectrum. Here,  $i_L$  and  $i_R$  are the centers of the left and right hole positions. Therefore, we can realize tunable Rabi oscillation in this hybrid system by changing the hole burning positions. Due to the small decay rate of the dark states, the Rabi splitting can even be observed in smaller spectral separation of hole positions centered at  $(i_L, i_R) = (22, 29)$ . In Fig. 2(d), we demonstrate the tunable Rabi oscillation by burning the spectral holes in symmetric positions centered at either  $(i_L, i_R) = (13, 38)$  or  $(i_L, i_R) = (19, 32)$  which are highlighted in the two white lines in Fig. 2(c). It is observed that the period of Rabi oscillation is changed which implies that the SHB not only suppresses the decoherence but also allows us to control the Rabi frequency by varying the positions of the spectral holes.

*constant and pulse drivings.*- Practically, people usually excite the system by a coherent constant field which can be modeled as  $E_L(t) = E_L$  in Eq. (1). In Fig. 3(a), we plot the quench dynamics for the photon population in the cavity after applying the constant field to demonstrate the SHB effect. The system is driven until it reaches the steady state, then we turn off the field and study how the system decays to its ground state. It is observed that the system does not excited efficiently even after the SHB. The cavity population decays rapidly either with or without the SHB. Alternatively, we can pump the system by a sequence of  $\pi$  phase-switched rectangular pulses, each with a period of  $T$  and a probing frequency  $\omega$  as shown in Fig. 3(c), this procedure is very efficient to feed energy into the hybrid system, leading to giant oscillation of cavity population [14, 20]. In Fig. 3(b), we optimize the maximal population of the cavity against the period and the probing frequency, finding that the population is optimal when the period is around the Rabi period,  $2\pi/\Omega$  and the probing frequency is on resonant with the frequencies of cavity and emitter,  $\omega = \omega_a = \omega_e$ . As displayed in Fig. 3(c), the maximal population for pulse driving is a magnitude larger than that for constant driving. For the SHB effect, not only the amplitude of driven oscillation is pronouncedly enhanced during the pumping, but also the relaxed oscillation after turning off the pulse is dramatically longer-lived than that without hole burning. The SHB effect is robust against the pulse period  $T$  and the probing fre-

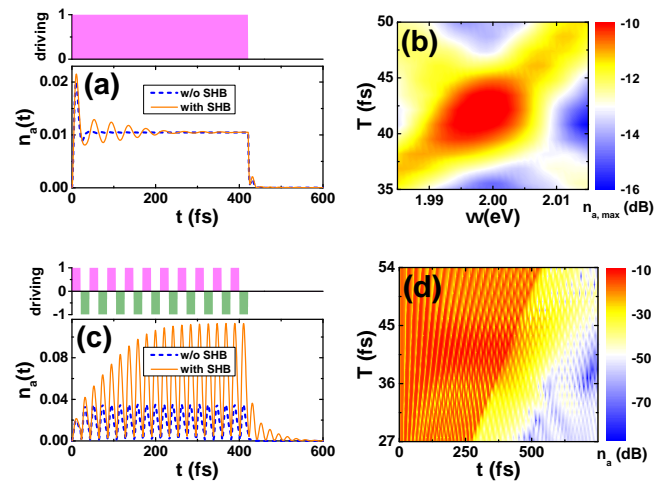


FIG. 3. dynamical response of cavity photon for different driving schemes. Both the cavity and emitters are initially prepared in their ground states. The parameters are the same as in Fig. 2(a). (a) SHB effect under a constant coherent driving. The driving is shown in the upper panel and the dynamics of cavity photon before and after SHB are shown in the lower panel. (b) Contour plot in the  $\omega \sim T$  plane to obtain the most efficient rectangular pulses for exciting the system. The best driving pulse is  $\omega = 2$  eV and  $T = 42$  fs. (c) SHB effect under a sequence of  $\pi$  phase-switched rectangular pulses. The driving field is shown in the upper panel and the dynamics of cavity photon before and after SHB are shown in the lower panel. (d) Contour plot in the  $t \sim T$  plane.

quency  $\omega$ . For instance, the SHB effect against the pulse period is shown in Fig. 3(d). We can see that the SHB effect can be clearly observed when the period ranges from 35 fs to 45 fs.

*Random effects.*- We now study the role of randomness in the SHB effect. First, we consider the imperfection of the frequency comb, where the emitter frequencies are not exactly located at the comb position. This imperfection can be modeled as a disorder among the transition frequencies of the comb, where the on-site energy of the emitters becomes  $H = \sum_i \omega'_i \sigma_i^+ \sigma_i^-$ . The imperfection is reflected in  $\omega'_i = \omega_i + \delta\omega_i$ , where  $\delta\omega_i = \alpha_i \Delta_{N-1}^\omega$  is a random on-site energy and the random number  $\alpha_i \in [-r, r]$  ( $0 \leq r < 1$ ) is uniformly distributed. Meanwhile, the corresponding coupling strength for each modified transition frequency follows the same  $q$ -Gaussian distribution  $g'_i = A e_q[-\beta(\omega'_i - \omega_e)^2]$ . In Fig. 4(a), we find that the SHB effect can be observed in the presence of the imperfection of the frequency comb.

Next we consider another case where the transition frequencies of emitters are randomly distributed by the  $q$ -Gaussian distribution and the couplings with plasmonic cavity are kept in constant for all the emitters. Particularly, we sample  $N = 5000$  emitters from the same  $q$ -Gaussian distribution parameterized by  $q = 2$  and  $\beta = 0.1$  and set the coupling strength of each emitter to be identical,  $g_i = 2$ . It is found in Fig. 4(b) that the SHB

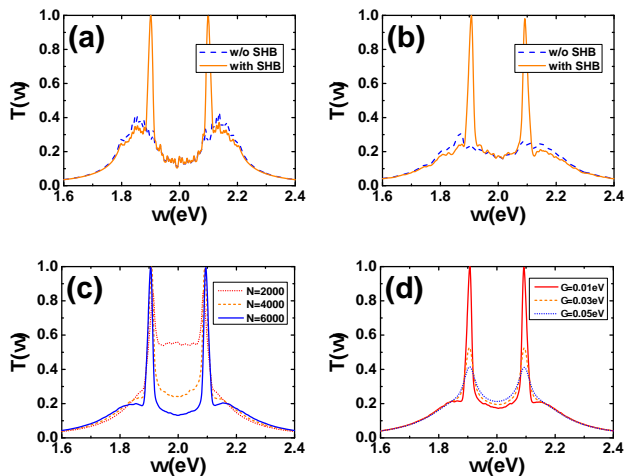


FIG. 4. Randomness in the SHB effect. (a) SHB effect for the imperfection of frequency comb. The parameters are the same as in Fig. 2(a) with  $r = 0.5$ . (b) SHB effect for a  $q$ -Gaussian randomly distributed ensemble with  $N = 5000$  emitters. The spectral holes are burned at  $\omega_L = 1.9$  eV and  $\omega_R = 2.1$  eV with width of 0.033 eV. (c) transmission function for SHB effect with different emitter numbers  $N = 2000, 4000, 6000$ . (d) transmission function for SHB effect with different decay rates  $\Gamma = 0.01, 0.03, 0.05$  eV.

effect can be observed in the dense emitter ensemble with individually weak coupling strength. The SHB effect will be in stronger contrast to the background spectrum when the number of emitters become larger. As shown in Fig. 4(c), the SHB effect become more and more significant

as the emitter number goes from 2000 to 6000. We also discuss the influence of fundamental decay rate to the SHB effect. For instance, when the decay rate of individual emitter  $\Gamma$  increases from 0.01eV to 0.05eV, the SHB effect will shrink gradually as seen in Fig. 4(d).

*Conclusion.*- In conclusion, we have demonstrated the SHB effect in the hybrid plasmonic system in the bad cavity region. We find that the coherent time of the Rabi oscillation of this hybrid system can be significantly increased by burning two narrow spectral holes in the spectral density of emitter ensemble where the transition frequencies are distributed in a frequency comb. The advantage for this comb setup is that the SHB effect can be observed in a small emitter ensemble ( $N \sim 50$ ) while a large emitter ensemble ( $N \sim 5000$ ) is needed for randomly-distributed transition frequencies. We then propose to observe the SHB effect by efficiently drive the system by a sequence of  $\pi$  phase-switched rectangular pulses. The imperfection of frequency comb and the ensemble with randomly-distributed transition frequencies are also discussed. The results show that the SHB effect is robust to the randomness. The SHB technique paves the way for practical use of quantum plasmonic systems in quantum information processing.

*acknowledgement.*- The IHPC A\*STAR Team acknowledge the support from the National Research Foundation Singapore (Grants No. NRF2017NRFNSFC002-015, No. NRF2016-NRF-ANR002, No. NRF-CRP 14-2014-04) and A\*STAR SERC (Grant No. A1685b0005). W.-L. Yang acknowledges financial supports from the Youth Innovation Promotion Association (CAS No. 2016299) and the National Natural Science Foundation of China (Grants No. 11574353).

- 
- [1] M. S. Tame, K. R. McEnery, S. K. Özdemir, J. Lee, S. A. Maier, and M. S. Kim, *Nature Physics* **9**, 329 (2013).
- [2] D. Xu, X. Xiong, L. Wu, X.-F. Ren, C. E. Png, G.-C. Guo, Q. Gong, and Y.-F. Xiao, *Adv. Opt. Photon.* **10**, 703 (2018).
- [3] D. K. Gramotnev and S. I. Bozhevolnyi, *Nature Photonics* **4**, 83 (2010).
- [4] J. A. Schuller, E. S. Barnard, W. Cai, Y. C. Jun, J. S. White, and M. L. Brongersma, *Nature Materials* **9**, 193 (2010).
- [5] K. Yao and Y. Liu, *Nanotechnology Reviews* **3**, 177 (2014).
- [6] N. Kongsuwan, X. Xiong, P. Bai, J.-B. You, C. E. Png, L. Wu, and O. Hess, *Nano Letters* **19**, 5853 (2019).
- [7] X. Xiong, J.-B. You, P. Bai, C. E. Png, Z.-K. Zhou, and L. Wu, *Nanophotonics* **0**, 0 (2019).
- [8] K. Santhosh, O. Bitton, L. Chuntonov, and G. Haran, *Nature Communications* **7**, 11823 (2016).
- [9] R. Chikkaraddy, B. de Nijs, F. Benz, S. J. Barrow, O. A. Scherman, E. Rosta, A. Demetriadou, P. Fox, O. Hess, and J. J. Baumberg, *Nature* **535**, 127 (2016).
- [10] R. Liu, Z.-K. Zhou, Y.-C. Yu, T. Zhang, H. Wang, G. Liu, Y. Wei, H. Chen, and X.-H. Wang, *Phys. Rev. Lett.* **118**, 237401 (2017).
- [11] Z. Kurucz, J. H. Wesenberg, and K. Mølmer, *Phys. Rev. A* **83**, 053852 (2011).
- [12] I. Diniz, S. Portolan, R. Ferreira, J. M. Gérard, P. Bertet, and A. Auffèves, *Phys. Rev. A* **84**, 063810 (2011).
- [13] D. O. Krimer, S. Putz, J. Majer, and S. Rotter, *Phys. Rev. A* **90**, 043852 (2014).
- [14] S. Putz, D. O. Krimer, R. Amsüss, A. Valookaran, T. Nöbauer, J. Schmiedmayer, S. Rotter, and J. Majer, *Nature Physics* **10**, 720 (2014).
- [15] S. Putz, A. Angerer, D. O. Krimer, R. Glattauer, W. J. Munro, S. Rotter, J. Schmiedmayer, and J. Majer, *Nature Photonics* **11**, 36 (2017).
- [16] H. Trommsdorff, A. Corval, and L. von Lau, *Pure & Appl. Chem.* **67**, 191 (1995).
- [17] U. P. Wild, S. E. Bucher, and F. A. Burkhalter, *Appl. Opt.* **24**, 1526 (1985).
- [18] J. Friedrich, H. Scheer, B. Zickendraht-Wendelstadt, and D. Haarer, *The Journal of Chemical Physics* **74**, 2260 (1981).
- [19] S.-Q. Kuang, P. Du, R.-G. Wan, Y. Jiang, and J.-Y. Gao, *Opt. Express* **16**, 11604 (2008).
- [20] D. O. Krimer, B. Hartl, and S. Rotter, *Phys. Rev. Lett.*

- [115](#), [033601](#) (2015).
- [21] R. Sáez-Blázquez, J. Feist, F. J. García-Vidal, and A. I. Fernández-Domínguez, [Phys. Rev. A](#) **98**, [013839](#) (2018).
- [22] H. S. Dhar, M. Zens, D. O. Krimer, and S. Rotter, [Phys. Rev. Lett.](#) **121**, [133601](#) (2018).
- [23] S. Umarov, C. Tsallis, and S. Steinberg, [Milan Journal of Mathematics](#) **76**, 307 (2008).
- [24] M. Fleischhauer, A. Imamoglu, and J. P. Marangos, [Rev. Mod. Phys.](#) **77**, [633](#) (2005).
- [25] U. Schollwöck, [Annals of Physics](#) **326**, [96](#) (2011).
- [26] F. Verstraete, V. Murg, and J. Cirac, [Advances in Physics](#) **57**, 143 (2008).
- [27] J. Cui, J. I. Cirac, and M. C. Bañuls, [Phys. Rev. Lett.](#) **114**, [220601](#) (2015).
- [28] E. Mascarenhas, H. Flayac, and V. Savona, [Phys. Rev. A](#) **92**, [022116](#) (2015).
- [29] J. del Pino, F. A. Y. N. Schröder, A. W. Chin, J. Feist, and F. J. Garcia-Vidal, [Phys. Rev. Lett.](#) **121**, [227401](#) (2018).
- [30] J. del Pino, F. A. Y. N. Schröder, A. W. Chin, J. Feist, and F. J. Garcia-Vidal, [Phys. Rev. B](#) **98**, [165416](#) (2018).
- [31] J. Haegeman, J. I. Cirac, T. J. Osborne, I. Pizorn, H. Verschelde, and F. Verstraete, [Phys. Rev. Lett.](#) **107**, [070601](#) (2011).
- [32] J. Haegeman, C. Lubich, I. Oseledets, B. Vandereycken, and F. Verstraete, [Phys. Rev. B](#) **94**, [165116](#) (2016).